

Lavinskyite-1M, $K(\text{LiCu})\text{Cu}_6(\text{Si}_4\text{O}_{11})_2(\text{OH})_4$, the monoclinic MDO equivalent of lavinskyite-2O (formerly lavinskyite), from the Cerchiara manganese mine, Liguria, Italy

UWE KOLITSCH^{1,2,*}, STEFANO MERLINO³, DONATO BELMONTE⁴, CRISTINA CARBONE⁴, ROBERTO CABELLA⁴, GABRIELLA LUCCHETTI⁴ and MARCO E. CIRIOTTI⁵

¹ Mineralogisch-Petrographische Abt., Naturhistorisches Museum, Burgring 7, 1010 Wien, Austria

*Corresponding author, e-mail: uwe.kolitsch@nhm-wien.ac.at

² Institut für Mineralogie und Kristallographie, Geozentrum, Universität Wien, Althanstraße 14, 1090 Wien, Austria

³ Università degli Studi di Pisa, Dipartimento di Scienze della Terra, Via S. Maria 53, 56126 Pisa, Italy

⁴ DISTAV, Università degli Studi di Genova, Corso Europa 26, 16132 Genova, Italy

⁵ Associazione Micromineralogica Italiana, Via San Pietro, 55, 10073 Devesi-Cirié, Italy

Abstract: Lavinskyite-1M, a monoclinic MDO (Maximum Degree of Order) polytype related to the orthorhombic MDO polytype lavinskyite-2O (formerly lavinskyite, now redefined), was identified in samples from the Cerchiara manganese mine (Liguria, Italy). Both polytypes have the same ideal chemical formula, $K(\text{LiCu})\text{Cu}_6(\text{Si}_4\text{O}_{11})_2(\text{OH})_4$. Lavinskyite-1M was originally approved as “liguriaite”, but was subsequently redefined as lavinskyite-1M (IMA proposal 16-E).

Lavinskyite-1M occurs as blue, micaceous aggregates embedded in calcite-filled microfractures and veinlets, where it is associated with calcite, quartz, norrishite and “schefferite” (a Mn-bearing variety of diopside). Lavinskyite-1M is translucent to transparent, bluish to pale blue in colour with a very pale blue to whitish streak and vitreous lustre; it is non-fluorescent. Individual, always indistinct platelets are up to ~0.15 mm in length. The crystals are tabular (100) and elongate along [001]. Lavinskyite-1M is brittle with perfect cleavage parallel to {100}, and uneven fracture. The estimated Mohs hardness is ~5. The calculated density is 3.613 g/cm³ (for empirical formula). Optically, it is biaxial positive, with $\alpha = 1.674(2)$; $\beta = 1.692(3)$ and $\gamma = 1.730(3)$; $2V_\gamma$ is very large, ~75° (est.), $2V_\gamma$ (calc.) = 70°. Pleochroism is moderate: X (pale) blue, Y pale blue and Z pale blue with faint greenish tint; absorption $X \geq Z \geq Y$. Orientation: $X \wedge a \sim 20^\circ$ (probably in obtuse beta), $Y = b$, $Z \sim c$; optical elongation is positive and the optical axis plane is parallel to (010). No dispersion was observed.

Chemical analysis (quantitative SEM-EDS and LA-ICP-MS) of two samples yielded the empirical formulae (based on 26 O atoms) $(\text{K}_{1.08}\Sigma_{1.08}(\text{Li}_{0.89}\text{Mg}_{0.36}\text{Cu}_{0.33}\text{Na}_{0.22}\text{Mn}^{2+}_{0.04})\Sigma_{1.86}\text{Cu}_{6.00}\text{Si}_{8.08}\text{O}_{22}(\text{OH})_4$ and $(\text{K}_{1.08}\Sigma_{1.08}(\text{Li}_{0.89}\text{Cu}_{0.35}\text{Mg}_{0.28}\text{Na}_{0.22}\text{Mn}^{2+}_{0.04})\Sigma_{1.78}\text{Cu}_{6.00}\text{Si}_{8.12}\text{O}_{22}(\text{OH})_4$. Strongest lines in the X-ray powder diffraction pattern are [d in Å (I_{calc}) hkl]: 10.216 (100) 100, 9.007 (20) 110, 4.934 (19) 210, 3.983 (19) 230, 3.353 (33) 310, 2.8693 (22) 241, 2.6155 (35) 161, 2.3719 (23) 20-2. The crystal structure has been solved, using single-crystal X-ray diffractometer data ($R_{\text{int}} = 4.60\%$), by direct methods and refined in space group $P2_1/c$ (no. 14) to $R1 = 5.10\%$ and $wR2_{\text{all}} = 13.92\%$ [1786 ‘observed’ reflections with $F_o > 4\sigma(F_o)$, 199 parameters]. Refined unit-cell parameters are: $a = 10.224(2)$, $b = 19.085(4)$, $c = 5.252(1)$ Å, $\beta = 92.23(3)^\circ$, $V = 1024.0(4)$ Å³ ($Z = 2$). The chemical composition and crystal structure are supported by micro-Raman spectra.

Lavinskyite-1M has a sheet structure consisting of corrugated brucite-like $(\text{CuO}_2)_n$ layers with amphibole-type $(\text{SiO}_3)_n$ chains joined to both their upper and lower surfaces. Adjacent complex sheets are linked by [5]-coordinated Li atoms and Cu atoms in square coordination (nearly planar) and interlayer K atoms. Lavinskyite-1M is isostructural with a hypothetical monoclinic MDO polytype of plancheite, not yet found in nature, while lavinskyite-2O is isostructural with plancheite. It appears that a complex and delicate interplay between the Li:Cu and Cu:Mg ratios (lower in lavinskyite-1M), along with an additional influence of impurity cations such as Na and different conditions of formation, results in a stabilisation of the 1M polytype. The origin of lavinskyite-1M can be related to a complex, multi-stage hydrothermal evolution of the primary Fe-Mn ore at Cerchiara, which experienced a diffuse alkali metasomatism under strongly oxidising conditions and produced mineral assemblages enriched in Na, K and Li, while providing also appreciable amounts of Ba, Sr, Ca and Cu.

Key-words: MDO polytype; lavinskyite-1M; copper silicate; crystal structure; Raman spectroscopy; manganese mine; Liguria; Italy.

1. Introduction

An unusual blue, micaceous mineral, collected in 2004 on the dumps of the Cerchiara manganese mine (eastern

Liguria, northern Apennines, Italy) by Mr Fabrizio Castellaro of Mezzanego, Genoa, Italy, was soon recognised as a new alkali copper silicate and briefly mentioned as an unidentified species “UK4” in Castellaro

(2008). Preliminary results (Carbone *et al.*, 2014) suggested the new mineral to be a monoclinic polymorph of (orthorhombic) lavinskyite (Yang *et al.*, 2014). The later proposed species name liguriaite was originally chosen in recognition of the mineral-rich region in which the type locality is located (it is in fact the Italian region with the highest density of mineral species). However, after the mineral and its name had been approved by the IMA Commission on New Minerals, Nomenclature and Classification (IMA 2014-035), the authors, on re-reading published information on the plancheite OD family, realised that “liguriaite” was probably a monoclinic MDO polytype of (orthorhombic) lavinskyite, a conclusion then confirmed by detailed calculations and comparisons done by one of us (S.M.) and a careful re-refinement of the crystal structure. A subsequent proposal to redefine “liguriaite” as lavinskyite-1*M* and type lavinskyite as lavinskyite-2*O* was approved in 2016 (IMA proposal 16-E). The naming of the polytypes is in line with joint IMA-IUCr recommendations (Guinier *et al.*, 1984).

The studied lavinskyite-1*M* material consists of two micromount-sized cotype specimens; the first one is preserved in the collection of the Dipartimento di Scienze della Terra, dell’Ambiente e della Vita (DISTAV), Università degli Studi di Genova, Italy (catalogue no. MO482). The second cotype is preserved in the collection of the Natural History Museum in Vienna, Austria (catalogue no. N 9733). The total amount of material comprises three micromount-sized specimens. The present article provides a description of lavinskyite-1*M* and its relation to lavinskyite-2*O* within the newly defined lavinskyite OD family.

2. Occurrence and paragenesis

At the Cerchiara manganese mine, lavinskyite-1*M* occurs in microfractures and veinlets cross-cutting Jurassic meta-cherts (Lucchetti *et al.*, 1988; Palenzona *et al.*, 1988). Associated minerals include calcite, quartz, norrishite and “schefferite” (a Mn-bearing variety of diopside).

Polyphase mineral assemblages in manganese ores occur within metacherts of the northern Apennine ophiolitic units (“Diaspri di Monte Alpe” Formation), which underwent prehnite-pumpellyite facies metamorphism ($P=2.5\pm 0.5$ kbar, $T=275\pm 25$ °C) followed by hydrothermal mobilisation along fractures under decreasing thermobaric conditions (Cabella *et al.*, 1991, 1998). Circulation of fluids along extensional fractures induced further concentration of dispersed elements such as Ba, Sr, As, V and Te, and allowed the genesis of a great variety of rare and new minerals, both at Cerchiara (e.g. Basso *et al.*, 1993, 1997, 2000; Cabella *et al.*, 1993) and the nearby manganese mines of Val Graveglia (e.g. Lucchetti *et al.*, 1981; Basso *et al.*, 2005, 2008; Bindi *et al.*, 2011, 2013; Carbone *et al.*, 2013; Ma *et al.*, 2014; Kampf *et al.*, 2017). Although manganese mineralisations at the Cerchiara mine share a common petrogenetic environment with those of Val Graveglia, there are some relevant differences. The presence of hematite, besides braunite, as the main

constituent of the ore body at Cerchiara suggests highly oxidising conditions of the minerogenetic environment. This would be confirmed by the secondary mineral parageneses at Cerchiara, which are dominated by Mn^{3+} - and Fe^{3+} -rich silicates such as aegirine, piemontite, namansilite, orientite–macfallite and cerchiarite (Lucchetti *et al.*, 1988; Basso *et al.*, 1989a, 1989b, 2000; Kampf *et al.*, 2013), at variance with the relatively reducing johannsenite-, rhodonite-bearing assemblages of Val Graveglia (Cabella *et al.*, 1991). The recent findings at Cerchiara mine of a V^{5+} -bearing mica, balestrite (Lepore *et al.*, 2015) and of manganiceladonite, a new Mn^{3+} end-member of the celadonite family (Lepore *et al.*, 2017), further support the evidence of a strongly oxidising character of the hydrothermal fluids responsible for the mobilisation and subsequent recrystallisation of the Fe-Mn ore. Finally, the manganese mineralisations at Cerchiara experienced a large hydrothermal metasomatism induced by diffuse interaction with alkali-rich fluids, which produced peculiar mineral assemblages enriched in Na, K and Li and provided also appreciable amounts of Ba, Sr, Ca and Cu, in strong analogy with similar assemblages described at the Bruce mine and Wessels mine (Transvaal Supergroup in the Kalahari Manganese Field, South Africa) (Gnos *et al.*, 2003; Tsikos & Moore, 2005a; Moore *et al.*, 2011) and Hoskins mine (New South Wales, Australia) (Ashley, 1986; Eggleton & Ashley, 1989). These metasomatic mineralisations, concentrated in veins and voids cross-cutting both the metacherts and the braunite–hematite ore, are represented by alkali-rich and oxidised parageneses including characteristic (Na, K, Li)-rich minerals such as aegirine, albite, balestrite, namansilite, pectolite–serandite, richterite, magnesio-arfvedsonite, sugilite, nambulite and norrishite (Lucchetti *et al.*, 1988; Cabella *et al.*, 1990; Palenzona & Selmi, 1990; Balestra, 2005; Balestra *et al.*, 2009; Lepore *et al.*, 2015). The origin of lavinskyite-1*M* can be related to this complex, multi-stage hydrothermal evolution of the primary Fe-Mn ore at Cerchiara.

3. Physical properties

Lavinskyite-1*M* forms millimetric blue aggregates of subparallel platy crystals in association with quartz, calcite (partly etched away with dilute acid) and “schefferite” (a Mn-bearing variety of diopside) in grey-pinkish fibrous aggregates (Fig. 1). The mineral is tabular on (100) and elongate along [001], confirmed by a single-crystal XRD study of the morphology using video-based modelling of the crystal faces with the help of a dedicated diffractometer software module. Individual, always indistinct platelets are up to ~0.15 mm in length. Although the platy crystals sometimes show a roughly rectangular outline, only the form {100} was clearly identified; other forms were not recognisable. No twinning was observed during any of our studies. Lavinskyite-1*M* is brittle with perfect cleavage parallel to {100}, and uneven fracture. The estimated Mohs hardness is ~5 (by comparison with its polytype lavinskyite-2*O*). The calculated density is 3.613 g/cm³ (for the empirical formula).



Fig. 1. Millimetric blue aggregates of lavinskyite-1M associated with quartz, calcite (partly etched away) and “schefferite” (a Mn-bearing variety of diopside) in grey-pinkish fibrous aggregates. Field of view 6 mm across. Photo Harald Schillhammer.

Optically, lavinskyite-1M is biaxial positive, with $\alpha = 1.674(2)$; $\beta = 1.692(3)$ and $\gamma = 1.730(3)$; $2V_\gamma$ is very large, $\sim 75^\circ$ (estimated using polarised-light microscopy), $2V_\gamma(\text{calc.}) = 70^\circ$. Pleochroism is moderate: X (pale) blue, Y pale blue and Z pale blue with faint greenish tint; absorption $X \geq Z \geq Y$. Orientation is: $X \wedge a \sim 20^\circ$ (probably in obtuse beta), $Y = b$, $Z \sim c$; optical elongation is positive and the optical axis plane is parallel to (010). No dispersion was observed. The mineral is insoluble in cold dilute HCl.

4. Chemical composition

Chemical analyses of two lavinskyite-1M samples (sectioned, polished and carbon-coated crystal aggregates) were carried out using a Tescan Vega 3 LMU scanning-electron microscope equipped with an energy-dispersive X-ray spectrometer (EDAX Apollo X SDD) and TEAM EDS (Texture and Elemental Analytical Microscopy) software (e-ZAF correction). Operating conditions were: voltage 20 kV, sample current 1.2 nA, beam diameter 320 nm, count rate 60 s. Standards used were: Metals MAC std for V and Fe, Wollastonite MAC std for Ca and Si, Orthoclase MAC std for K, Ilmenite USNM 96189 for Mn, Omphacite USNM 110607 for Mg and Chalcopyrite C23T for Cu. The mineral was stable under the electron beam. The analyses showed small variations within and between grains. Na and Li contents were measured separately by LA-ICP-MS. We point out that Ca, Sr or Ba were detected neither by SEM-EDS nor by EMP-WDS. The water content could not be determined directly due to the meagre quantity of material, and hence was added for charge balance ($\Sigma \text{cations} = +52.00$) and to bring the analytical total close to 100%. The chemical analyses of the two samples, listed in Table 1, yielded the empirical formulae (based on 26 O atoms) $(\text{K}_{1.08})_{\Sigma 1.08}(\text{Li}_{0.89}\text{Mg}_{0.36}\text{Cu}_{0.33}\text{Na}_{0.22}\text{Mn}^{2+}_{0.04})_{\Sigma 1.86}\text{Cu}_{6.00}\text{Si}_{8.08}\text{O}_{22}(\text{OH})_4$ and $(\text{K}_{1.08})_{\Sigma 1.08}(\text{Li}_{0.89}\text{Cu}_{0.35}\text{Mg}_{0.28}\text{Na}_{0.22}\text{Mn}^{2+}_{0.04})_{\Sigma 1.78}\text{Cu}_{6.00}\text{Si}_{8.12}\text{O}_{22}(\text{OH})_4$, *i.e.* very similar

compositions. The ideal chemical formula is $\text{K}(\text{LiCu})\text{Cu}_6(\text{Si}_4\text{O}_{11})_2(\text{OH})_4$, identical to that of its orthorhombic polytype lavinskyite-2O (Yang *et al.*, 2014, this work).

The Gladstone-Dale compatibility (Mandarino, 1981) is superior (-0.011) for the empirical formula.

5. Raman spectroscopy

Micro-Raman spectra (Fig. 2) were recorded on randomly oriented grains in the Raman shift range $100\text{--}4000\text{ cm}^{-1}$ using a Renishaw Ramascope equipped with a He-Ne laser (633 nm) and connected to a Leica optical microscope equipped with an Olympus SLM plan 20 \times long focal objective. The Raman spectra of lavinskyite-1M and lavinskyite-2O (Yang *et al.*, 2014, this work) are very similar in the low-wavenumber region and in the OH region. However, in the first region some peaks are less pronounced in lavinskyite-1M (region from 800 to 1200 cm^{-1}), and in the OH region lavinskyite-2O shows three bands at 3630 , 3662 and 3694 cm^{-1} (Yang *et al.*, 2014) whereas lavinskyite-1M has only two (at 3662 and 3694 cm^{-1}). These two bands are assigned to OH stretching vibrations, in accordance with the crystal-structure determination (see below). No bands indicating any presence of CO_3^{2-} were observed.

6. X-ray crystallography

The crystal structure was solved using single-crystal X-ray intensity data collected at ambient temperature from a suitable tiny crystal fragment on a Nonius KappaCCD single-crystal X-ray diffractometer equipped with a CCD detector and a $300\text{ }\mu\text{m}$ diameter capillary-optics collimator to provide increased resolution. The measured intensity data were processed with the Nonius program suite DENZO-SMN and corrected for Lorentz, polarisation, background and absorption effects, the latter by the multi-scan method (Otwinowski *et al.*, 2003). The crystal-structure solution employed direct methods (SHELXS-97, Sheldrick, 2008) in space group $P2_1/c$ (no. 14), as indicated by the observed systematic extinctions and intensity statistics. The model was smoothly refined by full-matrix least-squares techniques on F^2 (SHELXL-97, Sheldrick, 2008) to $R1 = 5.10\%$ and $wR2_{\text{all}} = 13.92\%$ [1786 ‘observed’ reflections with $F_o > 4\sigma(F_o)$, 199 parameters]. The topology obtained was identical to that of the orthorhombic polytype lavinskyite-2O (Yang *et al.*, 2014, this work). Specifically, the M4 site was found to be split in the same manner as in lavinskyite-2O, *i.e.* into an (ideally) half-occupied Cu site [M(4a)] and an (ideally) half-occupied Li site [M(4b)]. The occupancy of the Cu site, if freely refined, is $0.594(4)$, with an U_{eq} of $0.0217(5)\text{ \AA}^2$, only slightly higher than the U_{eq} values of the three remaining metal sites M1-3 occupied by Cu (and minor Mg). Free isotropic refinement of the Li site resulted in a physically unrealistic U_{iso} of 0.00001 \AA^2 and an occupancy of 0.23 . Therefore, U_{iso} was fixed to a reasonable value of 0.05 \AA^2 , resulting in a Li-site occupancy of $0.36(3)$. The

Table 1. Chemical-analytical data (wt%) for lavinskyite-1M.

Constituent	Cerch1 (7 points)			Cerch2 (7 points)			Probe standard
	Wt%	Range	SD	Wt%	Range	SD	
SiO ₂	42.51	40.94–45.37	1.31	42.98	42.20–43.41	0.44	wollastonite
CuO	44.12	40.69–45.97	1.77	44.53	43.71–45.78	0.66	chalcopyrite
MgO	1.27	0.26–3.76	1.21	0.99	0.00–1.90	0.65	omphacite
MnO	0.27	0.21–0.38	0.07	0.23	0.00–0.32	0.10	metallic Mn
Na ₂ O*	0.61	0.55–0.70	0.05	0.61	0.55–0.70	0.05	–
K ₂ O	4.46	4.37–4.58	0.07	4.48	4.39–4.59	0.07	orthoclase
Li ₂ O*	1.17	1.10–1.26	0.05	1.17	1.10–1.26	0.05	–
H ₂ O**	3.16			3.18			–
Total	97.58			98.29			

* Measured separately by LA-ICP-MS (average values, 12 data points). Na was also measured by EPMA-WDS and gave 0.66 wt% Na₂O on average, close to the average value of 0.61 wt% Na₂O obtained by LA-ICP-MS.

** Water added for charge balance ($\Sigma\text{cations} = +52.00$) and to bring analytical total close to 100%.

Ca, Sr or Ba were neither detected by SEM-EDS nor by EMPA-WDS.

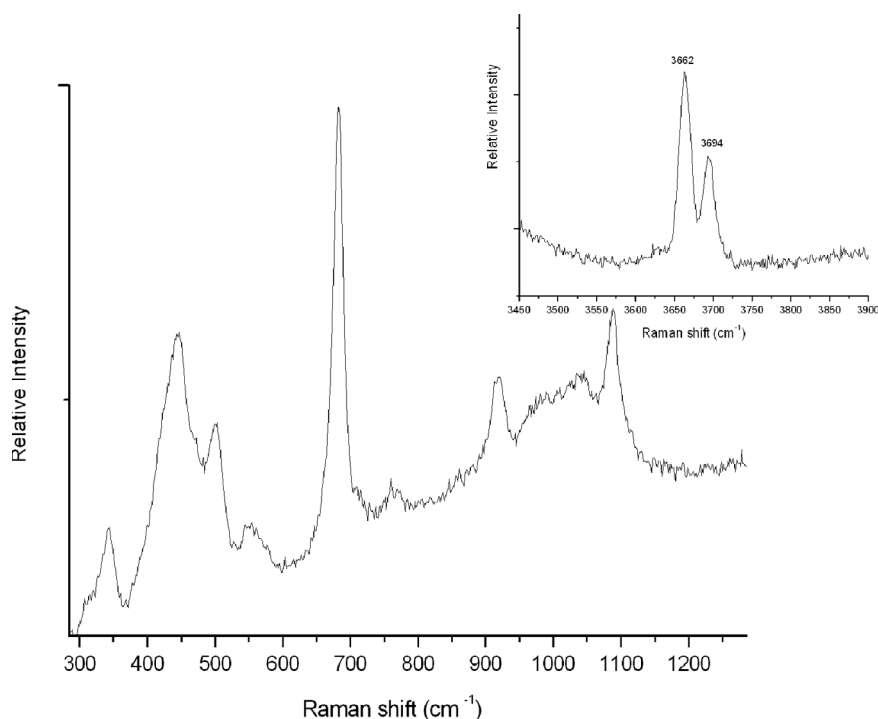


Fig. 2. Single-crystal laser-Raman spectrum of lavinskyite-1M in the low-wavenumber region ($<1300\text{ cm}^{-1}$) and in the O-H stretching region (inset).

latter is reasonably close to the ideal value of 0.5, considering the low electron density involved and the imperfect quality of the dataset. If the Li-atom coordinates were refined with a fixed U_{iso} of 0.05 \AA^2 and freely variable occupancy, the following values were obtained: 0.098(4), 0.796(2), 0.157(8). In contrast, for a fixed half-occupancy, the coordinates refined to 0.106(9), 0.748(5), 0.26(2), *i.e.* values with approximately doubled s.u.s, and the $M(4a)$ – $M(4b)$ distance was unrealistically short ($\sim 0.06\text{ \AA}$); furthermore, the value for $(\Delta/\sigma)_{\text{max}}$ in the refinement was ~ 1.00 , again unrealistic and far from

the commonly observed value of ~ 0.00 . Consequently, the coordinates were fixed to those obtained from the refinement with freely variable occupancy, which resulted in a much more reasonable $(\Delta/\sigma)_{\text{max}}$ of 0.000 and a $M(4a)$ – $M(4b)$ distance similar to that in lavinskyite-2O ($\sim 1.0\text{ \AA}$, for details see below). In the final model, the occupancies of both $M(4a)$ and $M(4b)$ were fixed to 0.5, to obtain a charge-balanced formula. Note, however, that, firstly, this increased the $R(F)$ value from 4.8% to 5.1%. Secondly, the freely refined occupancies of the $M(4a)$ and $M(4b)$ sites, 0.594(4) and 0.36(3), would result

Table 2. Crystal data, data collection information and refinement details for lavinskyite-1M.

Crystal data	
Formula (idealised)	$\text{K}(\text{LiCu})_{\Sigma 2}(\text{Cu}_{4.41}\text{Mg}_{1.59})_{\Sigma 6}(\text{Si}_4\text{O}_{11})_2(\text{OH})_4$
Formula weight	1087.17
Space group, Z	$P2_1/c$ (no. 14), 2
a, b, c (Å)	10.224(2), 19.085(4), 5.252(1)
β (°)	92.23(3)°
V (Å ³)	1024.0(4)
$F(000)$, ρ_{calc} (g cm ⁻³)	1044, 3.480
μ (mm ⁻¹)	6.375
Absorption correction	multi-scan (Otwinowski <i>et al.</i> , 2003)
Crystal dimensions (mm)	0.015 × 0.05 × 0.10 mm
Data collection and refinement	
Diffractometer	Nonius KappaCCD system
λ (Mo-K α) (Å), T (K)	0.71073, 293
Crystal-detector distance	34 mm
Rotation axis, width (°)	$\phi, \omega, 1$
Total no. of frames	914
Collect. time per frame (s)	370
Collection mode, $2\theta_{\text{max}}$ (°)	sphere, 60
h, k, l ranges	-13→13, -25→25, -7→7
Total reflections measured	5072
Unique reflections	2619 ($R_{\text{int}} = 4.60\%$)
Refinement on	F^2
$R1(F)$, $wR2_{\text{all}}(F^2)^*$	5.10%, 13.92%
'Observed' reffs.	1786 [$F_o > 4\sigma(F_o)$]
Extinct. coefficient	0.0
No. of refined parameters	199
GooF	1.056
$(\Delta/\sigma)_{\text{max}}$	0.000
$\Delta\rho_{\text{min}}, \Delta\rho_{\text{max}}$ (e/Å ³)	-1.11, 1.42

Unit-cell parameters were refined from 3003 recorded reflections. Scattering factors for neutral atoms were employed in the refinement.

* $w = 1/[\sigma^2(F_o^2) + (0.0787P)^2 + 0.0P]$; $P = ([\text{max of } (0 \text{ or } F_o^2)] + 2F_c^2)/3$.

in a total positive charge of 1.55+, very close to the ideal value of 1.50+ for a 50:50 occupancy. For further details on the topological environment of these two sites, see the discussion below.

Prior to the final refinement step, the coordinates were standardised using STRUCTURE TIDY (Gelato & Parthé, 1987), and the metal-atom labelling was adopted from the structure description of lavinskyite-2O (Yang *et al.*, 2014). Version 1.16 of PLATON (Spek, 2003, 2009) confirmed the space-group choice and the validity of the structure model. Detailed information about the crystal data, data collection and refinement are presented in Table 2. Table 3 contains atomic coordinates and equivalent isotropic displacement parameters, the anisotropic ones are given in Table 4 (deposited, *i.e.* freely available as Supplementary Material linked to this article on the GSW website of the journal: <https://pubs.geoscienceworld.org/eurjmin>). Selected geometric parameters are provided in Table 5. Due to the meagre amount of available material, indexed X-ray powder diffraction data (Table 6, deposited) were calculated from the crystal-structure model.

Table 3. Fractional atomic coordinates and displacement parameters (Å²) for lavinskyite-1M. U_{eq} according to Fischer & Tillmanns (1988).

Atom*	x	y	z	$U_{\text{eq}}/U_{\text{iso}}$
K	0.0	0.0	0.5	0.0371(6)
$M(1)$	0.48692(10)	0.04036(5)	0.24540(18)	0.0141(4)
$M(2)$	0.44601(7)	0.37560(4)	0.21827(14)	0.0140(3)
$M(3)$	0.39742(8)	0.20720(4)	0.19849(14)	0.0145(3)
$M(4a)$	0.10774(13)	0.75060(7)	0.2659(3)	0.0133(3)
$M(4b)$	0.0980	0.7960	0.1570	0.050
Si(1)	0.28234(16)	0.64186(9)	0.0527(3)	0.0168(4)
Si(2)	0.25634(16)	0.56241(8)	0.5484(3)	0.0165(4)
Si(3)	0.18579(16)	0.09385(8)	0.0041(3)	0.0169(4)
Si(4)	0.13786(17)	0.17167(8)	0.4929(3)	0.0172(4)
O(1)	0.5623(4)	0.1279(2)	0.4261(8)	0.0185(9)
O(2)	0.2462(5)	0.7234(2)	0.0261(9)	0.0264(10)
O(3)	0.2138(4)	0.6121(2)	0.3086(8)	0.0232(10)
O(4)	0.7894(4)	0.4010(2)	0.1894(8)	0.0240(10)
O(5)	0.5907(4)	0.4535(2)	0.4388(7)	0.0186(9)
O(6)	0.1685(4)	0.0088(2)	0.0126(8)	0.0230(10)
O(7)	0.1064(4)	0.1208(2)	0.2456(8)	0.0225(10)
O(8)	0.3373(4)	0.1191(2)	0.0247(8)	0.0183(9)
O(9)	0.1178(4)	0.3824(2)	0.2340(8)	0.0237(10)
O(10)	0.2851(4)	0.2003(2)	0.4889(8)	0.0214(10)
O(11)	0.0251(5)	0.2707(2)	0.0028(9)	0.0299(11)
Oh(12)	0.3791(4)	0.4612(2)	0.0492(8)	0.0208(9)
Oh(13)	0.4980(4)	0.2853(2)	0.3842(7)	0.0176(9)

Oxygen atoms of hydroxyl groups are designated as Oh.

* Refined occupancies of mixed sites: $M(1) = \text{Cu}_{0.455(6)}\text{Mg}_{0.546(6)}$, $M(2) = \text{Cu}_{0.825(6)}\text{Mg}_{0.175(6)}$ and $M(3) = \text{Cu}_{0.869(6)}\text{Mg}_{0.131(6)}$; the occupancies of the Cu [$M(4a)$] and Li [$M(4b)$] site were fixed to 0.5 and the coordinates of the nearly half-occupied, isotropically refined Li site [$M(4b)$] were fixed (see text).

7. Derivation and description of the lavinskyite OD family

In their original description of lavinskyite, Yang *et al.* (2014) stressed the close relationship of lavinskyite with isostructural plancheite (Evans & Mrose, 1977) and indicated that the only substantial differences are in the coupled substitutions of K^+ for H_2O and Li^+ for one half of the fourfold coordinated Cu^{2+} . We may add that, as it happens in plancheite (Merlino, 1997; Ferraris *et al.*, 2004), lavinskyite, too, displays OD (Dornberger-Schiff, 1964, 1966; Ferraris *et al.*, 2004) character.

Lavinskyite is built up by two distinct structural layers, both with translation vectors \mathbf{b}, \mathbf{c} ($b = 19.046$, $c = 5.2497$ Å) regularly alternating in the \mathbf{a}_0 direction ($a_0 = 10.1885$ Å); note that we have exchanged the \mathbf{a} and \mathbf{b} directions with respect to the choice of Yang *et al.* (2014). The first layer is constituted by the complex TOT block, with brucite-like CuO_2 sheets sandwiched by amphibole-like chains on both sides, and by Li^+ cations (L_{2n} layers, with symmetry $P2_1/c$); the second layer – separated from the previous one by undulating border-planes – is constituted by half-occupied ladder-like ribbons of copper atoms in (nearly) square coordination running along \mathbf{c} and by K^+ cations (L_{2n+1} layer with layer symmetry $Pn\text{cm}$).

Table 5. Selected geometric parameters (Å) for the coordination polyhedra in lavinskyite-1*M*.

<i>M</i> (1)–O(5)	1.966(4)	Si(1)–O(2)	1.605(5)
<i>M</i> (1)–Oh(12)	1.974(4)	Si(1)–O(1)	1.610(4)
<i>M</i> (1)–O(1)	2.056(4)	Si(1)–O(3)	1.641(4)
<i>M</i> (1)–O(5)	2.063(4)	Si(1)–O(4)	1.658(5)
<i>M</i> (1)–Oh(12)	2.282(4)	<Si(1)–O>	1.629
<i>M</i> (1)–O(8)	2.409(4)		
< <i>M</i> (1)–O>	2.125		
<i>M</i> (2)–O(12)	1.969(4)	Si(2)–O(5)	1.592(4)
<i>M</i> (2)–O(1)	1.979(4)	Si(2)–O(3)	1.622(5)
<i>M</i> (2)–Oh(13)	1.994(4)	Si(2)–O(4)	1.629(4)
<i>M</i> (2)–O(8)	1.994(4)	Si(2)–O(6)	1.635(4)
<i>M</i> (2)–O(5)	2.368(4)	<Si(2)–O>	1.620
<i>M</i> (2)–O(10)	2.470(4)		
< <i>M</i> (2)–O>	2.129		
<i>M</i> (3)–O(10)	1.949(4)	Si(3)–O(7)	1.616(4)
<i>M</i> (3)–Oh(13) ¹	1.984(4)	Si(3)–O(9)	1.620(4)
<i>M</i> (3)–O(8)	1.999(4)	Si(3)–O(8)	1.622(4)
<i>M</i> (3)–Oh(13)	2.038(4)	Si(3)–O(6)	1.635(4)
<i>M</i> (3)–O(10) ¹	2.356(4)	<Si(3)–O>	1.623
<i>M</i> (3)–O(1)	2.531(4)		
< <i>M</i> (3)–O>	2.143		
<i>M</i> (4a)–O(11)	1.896(4)	Si(4)–O(11)	1.596(5)
<i>M</i> (4a)–O(11)	1.963(4)	Si(4)–O(10)	1.602(5)
<i>M</i> (4a)–O(2) ¹	1.992(4)	Si(4)–O(7)	1.644(4)
<i>M</i> (4a)–O(2)	2.000(4)	Si(4)–O(9)	1.652(4)
[<i>M</i> (4a)–O(3)]	[2.863(4)]	<Si(4)–O>	1.624
[<i>M</i> (4a)–O(4)]	[3.063(4)]		
< ^[4] <i>M</i> (4a)–O>	1.963		
<i>M</i> (4b)–O(11) ¹	1.956(5)	K–O(9) × 2	2.808(4)
<i>M</i> (4b)–O(2)	2.184(5)	K–O(7) × 2	2.897(4)
<i>M</i> (4b)–O(11)	2.277(5)	K–O(4) × 2	3.061(4)
<i>M</i> (4b)–O(4)	2.433(4)	K–O(6) × 2	3.144(4)
<i>M</i> (4b)–O(2) ¹	2.442(5)	K–O(6) × 2	3.145(4)
< ^[5] <i>M</i> (4b)–O>	2.258	[K–O(3) × 2]	[3.421(4)]
		< ^[10] K–O>	3.011
<i>M</i> (4a)– <i>M</i> (4b)	1.0410(14)		
Possible hydrogen bonds			
Oh(12)···O(9)	3.25		
Oh(13)···O(2)	2.89		

The fact that the symmetry of the L_{2n+1} layer is higher than that of L_{2n} layer points to the possibility of polytypic relationships. In the orthorhombic structure of lavinskyite, L_{2n} and L_{2n+2} layers are related through the glide operators $[n--]$ (and twofold operator $[-2]$) which convert the layer L_{2n+1} , lying between them, into itself: thus the pair $(L_{2n}; L_{2n+1})$ is converted by those operators into the pair $(L_{2n+2}; L_{2n+1})$. However, because of the symmetry displayed by the L_{2n+1} layer, a different arrangement is also possible. In this arrangement the layers L_{2n} and L_{2n+2} are related through the operators $[-2_1 -]$ (and the inversion centres) which convert the layer L_{2n+1} , lying between them, into itself. As in the preceding case, the pair $(L_{2n}; L_{2n+1})$ is converted by these operations into the pair $(L_{2n+2}; L_{2n+1})$.

Infinite ordered polytypes and disordered structures are possible, corresponding to the various possible sequences of operators that may be active in the L_{2n+1} layers. In all

of them pairs of adjacent layers are geometrically equivalent (*principle of OD structures*). The symmetry relations common to all the polytypes of the family are indicated by the OD groupoid family symbol:

$$P(1) 2_1/c 1 \quad P(2/n) 2_1/c 2/m \\ [0.0, -0.0375]$$

The first line presents the layer-group symmetry of the two kinds of layer, whereas the second line presents their positional relations, which is done giving in brackets the r and s components of the projection into the layer of the vector connecting the origins of the two subsequent layers (the values of r and s are referred to the basis vectors \mathbf{b} and \mathbf{c} of the common translation group).

Only one kind of $(L_{2n-1}; L_{2n}; L_{2n+1})$ triples exists, whereas there are two kinds of $(L_{2n}; L_{2n+1}; L_{2n+2})$ triples. Consequently the minimum number of different triples is 2 and only two MDO (Maximum Degree of Order) polytypes are possible, just corresponding to those polytypes presenting the minimum number of different triples of layers (*principle of MDO structures*).

In the first of them the glide $[n--]$ and the twofold axes $[-2]$ are constantly active in the L_{2n+1} layers; the generating operation is a glide normal to \mathbf{c} with translational component \mathbf{a}_0 ; the constant application of this operation generates an orthorhombic structure with basis vectors $\mathbf{a} = 2\mathbf{a}_0$, \mathbf{b} , \mathbf{c} and space-group symmetry $Pnca$, corresponding to the type lavinskyite studied by Yang *et al.* (2014) after the exchange of \mathbf{a} and \mathbf{b} vectors: the $[-a]$ glide corresponds to the generating operation, the $[-c-]$ glide is the common symmetry element of both OD layers, the $[n--]$ mirror of the L_{2n+1} layers is valid for the whole structure.

In the second MDO structure the operators $[-2_1 -]$ and inversion centres are constantly active in the L_{2n+1} layer. The generating operation is the translation $\mathbf{t} = \mathbf{a}_0 + 2s\mathbf{c}$ ($s = -0.0375$). The continuation of this operation gives rise to a monoclinic polytype with space-group symmetry $P2_1/c$ and basis vectors $\mathbf{a} = \mathbf{a}_0 + 2s\mathbf{c}$, \mathbf{b} , \mathbf{c} ($a = 10.196$, $b = 19.046$, $c = 5.2497$ Å, $\beta = 92.22^\circ$). These unit-cell parameters are closely similar to those obtained by Kolitsch *et al.* (2014) for the originally approved “liguriaite” (IMA 2014-035): $a = 10.224$, $b = 19.085$, $c = 5.252$ Å, $\beta = 92.23^\circ$.

8. Description of the crystal structure

A comparison of the crystal structures of lavinskyite-1*M* and lavinskyite-2*O* along two major axes is given in Fig. 3. The asymmetric unit of lavinskyite-1*M* contains three (Cu, Mg) [*M*(1), *M*(2), *M*(3)], one split Cu/Li [*M*(4)], one K, four Si, 13 O and two H sites (the latter could not be located). All atoms are in general positions except K which is located at (0, 0, 0.5). The atomic arrangement of lavinskyite-1*M* (Fig. 3a, b) is best described as a sheet structure consisting of corrugated brucite-like $(\text{CuO}_2)_n$ layers with amphibole-type $(\text{SiO}_3)_n$ chains joined to both their upper and lower surfaces. Adjacent complex sheets

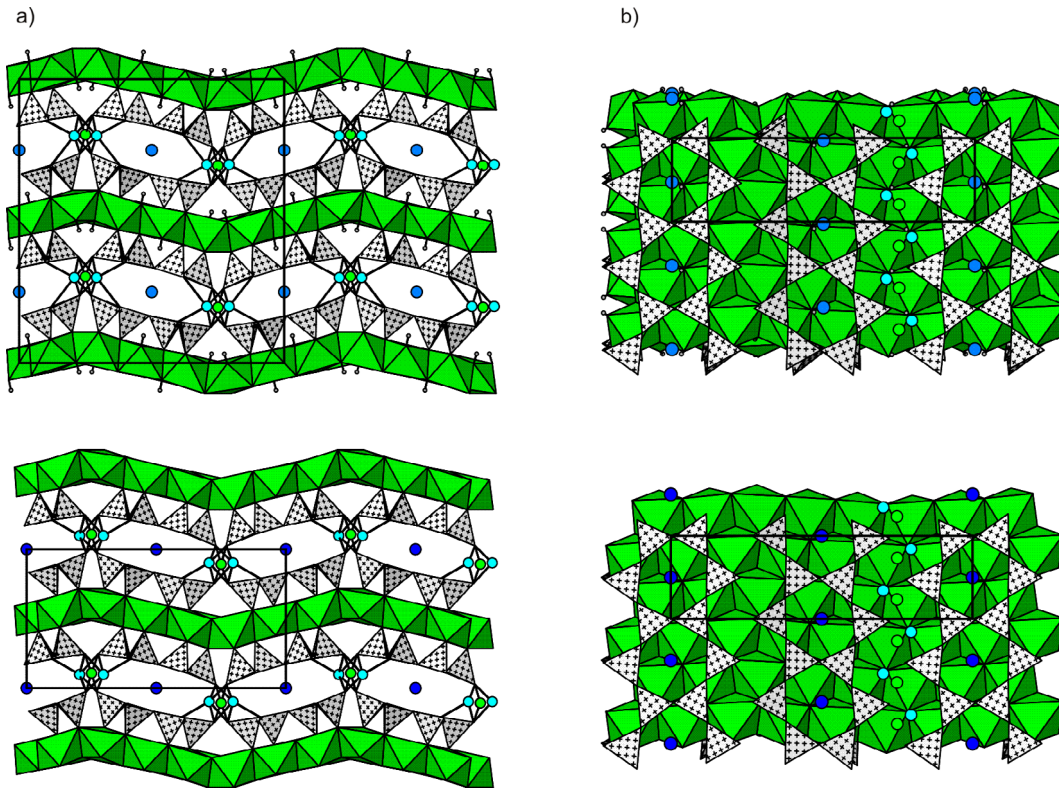


Fig. 3. Comparison of the crystal structures of lavinskyite-1*M* (bottom part) and lavinskyite-2*O* (top part). (a) View parallel to the corrugated brucite-like $(\text{CuO}_2)_n$ layers, along c ; (b) view perpendicular to the layers, along b (lavinskyite-2*O*) and $-a$ (lavinskyite-1*M*). Distorted MO_6 ($M = \text{Cu}, \text{Mg}$) octahedra are green; the split $M(4)$ site in both polytypes is represented by a green Cu sphere and a turquoise Li sphere, both shown with bonds in part (a) of the figure; SiO_4 tetrahedra are white and marked with crosses; K atoms are shown as dark blue spheres and H atoms as small grey spheres. The unit cells are outlined. Drawings done using ATOMS version 6.3 (Shape Software, 2006). (Online version in color)

are linked by [5]-coordinated Li atoms and Cu atoms in square coordination (nearly planar) and interlayer K atoms. The K site is fully occupied by K.

The three (Cu,Mg) sites $M(1)$, $M(2)$ and $M(3)$ show refined occupancies of $\text{Cu}_{0.455(6)}\text{Mg}_{0.546(6)}$, $\text{Cu}_{0.825(6)}\text{Mg}_{0.175(6)}$ and $\text{Cu}_{0.869(6)}\text{Mg}_{0.131(6)}$, respectively. Although the refinement suggests that Mg is very slightly dominant at the $M(1)$ site, the true experimental error of the refined Cu:Mg ratio is certainly higher (both the omission of several poorly fitting low-angle reflections and the treatment of the split $M4$ site had a large impact on this ratio, for example) and, consequently, there is no unambiguous proof for the dominance. The split Cu/Li [$M(4)$] site shows ideal occupancies of 0.5 for both Cu [$M(4a)$] and Li [$M(4b)$]. The same ideal occupancies characterise lavinskyite-2*O* (Yang *et al.*, 2014), in which $M(4a)$ – $M(4b)$ ~ 0.9 Å, similar to the equivalent distance in lavinskyite-1*M*, 1.0410(14) Å.

From a purely topological point of view, the position of the Li atom in lavinskyite-1*M* was found to be very close to that in lavinskyite-2*O* (Yang *et al.*, 2014). To quantify this closeness, detailed MDO-geometrical calculations were performed to obtain the coordinates of atoms in lavinskyite-1*M* from those in lavinskyite-2*O* (for details see Appendix in Supplementary Material). The calculated Li-atom coordinates (0.102, 0.792, 0.154) are very near to those found independently and then refined with fixed U_{iso} of 0.05 \AA^2 and freely refined occupancy: 0.098(4), 0.796

(2), 0.157(8). As mentioned above, the freely refined Li-atom occupancy in lavinskyite-1*M* is 0.36(3), reasonably close to the ideal value of 0.5, considering the low electron density involved and the imperfect quality of the dataset. The Li atom has five O ligands within a Li–O bond-length range of 1.96–2.44 Å (sixth and seventh neighbours would both be at 2.83 Å). The coordination is thus somewhat different from that in lavinskyite-2*O*, in which the Li atom shows a markedly distorted octahedral coordination, with Li–O bonds ranging from 1.91 to 2.70 Å. The coordination of the Li atom in both lavinskyite-1*M* and –2*O* is within the range reported for Li^+ (coordination numbers 3–8; Wenger & Armbruster, 1991). The Cu [$M(4a)$] site in lavinskyite-1*M* displays a distorted (nearly) planar four-coordinated environment very similar to that in lavinskyite-2*O*. The mentioned small differences in Li coordination number (six in lavinskyite-2*O* vs. five in lavinskyite-1*M*), in Li:Cu ratios and (Cu,Mg) site occupancies are thought to be the main reasons for the slight monoclinic lattice distortion of the 1*M* polytype (deviation from orthogonality $\sim 2.2^\circ$).

Lavinskyite-1*M* thus has the same topology as orthorhombic lavinskyite-2*O* [$\text{K}(\text{LiCu})\text{Cu}_6(\text{Si}_4\text{O}_{11})_2(\text{OH})_4$, *Pcnb* (Yang *et al.*, 2014, this work)], which is isostructural with plancheite (Evans & Mrose, 1977). The close relation between lavinskyite-1*M* and lavinskyite-2*O* is also evident from their unit-cell parameters:

Table 7. Comparison of physico-chemical data for lavinskyite-1*M*, lavinskyite-2*O* and plancheite.

Mineral	Lavinskyite-1 <i>M</i>	Lavinskyite-2 <i>O</i>	Plancheite
Ref.	This work	Yang <i>et al.</i> (2014), this work	Evans & Mrose (1977)
Formula	K(Li,Cu)Cu ₆ (Si ₄ O ₁₁) ₂ (OH) ₄	K(LiCu)Cu ₆ (Si ₄ O ₁₁) ₂ (OH) ₄	Cu ₈ (Si ₄ O ₁₁) ₂ (OH) ₄ · H ₂ O
Empirical formulae (both based on 26 O apfu)	(K _{1.08} Σ _{1.08} (Li _{0.89} Mg _{0.36} Cu _{0.33} Na _{0.22} Mn ²⁺ _{0.04})Σ _{1.84} Cu _{6.00} Si _{8.08} O ₂₂ (OH) _{4.02} and (K _{1.08} Σ _{1.08} (Li _{0.89} Cu _{0.33} Mg _{0.28} Na _{0.22} Mn ²⁺ _{0.04})Σ _{1.76} Cu _{6.00} Si _{8.09} O ₂₂ (OH) _{4.14})	(K _{0.99} Ba _{0.01})Σ _{1.00} (Li _{1.04} Cu _{0.93} Na _{0.10})Σ _{2.07} (Cu _{5.57} Mg _{0.43} Mn _{0.01})Σ _{6.01} (Si _{4.00} O ₁₁) ₂ (OH) ₄	–
Symmetry	Monoclinic	Orthorhombic	Orthorhombic
Space group	<i>P</i> 2 ₁ / <i>c</i>	<i>P</i> <i>c</i> <i>n</i> <i>b</i>	<i>P</i> <i>c</i> <i>n</i> <i>b</i>
<i>a</i> (Å)	10.224(2)	19.046(2)	19.043(3)
<i>b</i> (Å)	19.085(4)	20.377(2)	20.129(5)
<i>c</i> (Å)	5.252(1)	5.2497(6)	5.269(1)
β (°)	92.23(3)		
<i>V</i> (Å ³)	1024.0(4)	2037.4(4)	2019.7
<i>Z</i>	2	4	4
8 strongest lines in the powder pattern	10.216 (100), 9.007 (20), 4.934 (19), 3.983 (19), 3.353 (33), 2.869 (22), 2.616 (35), 2.372 (23)	10.189 (100), 8.984 (17), 4.921 (25), 3.973 (19), 3.343 (32), 2.693 (29), 2.522 (27), 2.316 (22)	10.11 (100), 9.56 (40), 6.94 (70), 4.87 (50), 4.06 (85), 3.95 (40), 3.31 (40)
<i>D</i> (meas.); (calc.)	n.d.; 3.613 (<i>D</i> _x 3.526)	3.61(3); 3.62	3.65-3.80; (<i>D</i> _x 3.815)
Mohs hardness	~5	~5	6
α	1.674(2)	1.675(1)	1.697
β	1.692(3)	1.686(1)	1.718
γ	1.730(3)	1.715(1)	1.741
Birefringence	0.056	0.040	0.044
Opt. character	2 (+)	2 (+)	2 (+)
2 <i>V</i> (meas.); (calc.)	~75°; 70°	64(4)°; 64.2°	n.d.; 88.5°
Dispersion	None	n.g.	n.g.
Orientation	<i>X</i> ^ <i>a</i> ~ 20° (in obtuse beta?), <i>Y</i> = <i>b</i> , <i>Z</i> ~ <i>c</i>	<i>X</i> = <i>a</i> , <i>Y</i> = <i>b</i> , <i>Z</i> = <i>c</i>	<i>X</i> = <i>c</i> , <i>Y</i> = <i>b</i> , <i>Z</i> = <i>a</i>
Elongation	Positive	n.g.	Positive
<i>X</i> (colour)	(Pale) blue	Dark blue	Very pale blue
<i>Y</i> (colour)	Pale blue	Light blue	Blue
<i>Z</i> (colour)	Pale blue with faint greenish tint	Light blue	Blue
Absorption	<i>X</i> ≥ <i>Z</i> ≥ <i>Y</i>	<i>X</i> > <i>Y</i> = <i>Z</i>	<i>Z</i> > <i>X</i> > <i>Y</i>
Megascopic colour	Bluish, pale blue	Light blue	Pale blue to deep blue, pale greenish blue
Lustre	Vitreous	Vitreous	Satiny
Streak	Very pale blue to white	Very pale blue	Light blue
Habit	Tabular (100), elongated [001]	Tabular (010), elongated [001]	Fibrous [001]
Twinning	None observed	None observed	None observed
Cleavage	Perfect {100}	Perfect {010}	n.g.
Fracture	Uneven	Uneven	n.g.

* Plancheite: Data from Handbook of Mineralogy (<http://rruff.info/doclib/hom/plancheite.pdf>) and Lacroix (1908).

Lavinskyite-1*M*: *a* = 10.224(2), *b* = 19.085(4), *c* = 5.252(1) Å, β = 92.23(3)°, *V* = 1024.0(4) Å³.

Lavinskyite-2*O*: *a* = 19.046(2), *b* = 20.377(2), *c* = 5.2497(6) Å, *V* = 2037.4(4) Å³.

The comparison shows that $a_{L1M} \sin \beta_{L1M} \sim 0.5b_{L2O}$, $b_{L1M} \sim a_{L2O}$, $c_{L1M} \sim c_{L2O}$ and $V_{L1M} \sim 0.5V_{L2O}$.

Lavinskyite-1*M* and lavinskyite-2*O* have nearly the same empirical formula: (K_{1.08})Σ_{1.08}(Li_{0.89}Mg_{0.36}Cu_{0.33}Na_{0.22}Mn²⁺_{0.04})Σ_{1.84}Cu_{6.00}Si_{8.08}O₂₂(OH)_{4.02} and (K_{0.99}Ba_{0.01})Σ_{1.00}(Li_{1.04}Cu_{0.93}Na_{0.10})Σ_{2.07}(Cu_{5.57}Mg_{0.43}Mn_{0.01})Σ_{6.01}(Si_{4.00}O₁₁)₂(OH)₄, respectively. The chemical formula

obtained from the structure refinement of lavinskyite-1*M* (neglecting the minor Na and the trace amounts of Mn) is: K(LiCu)_{Σ2}(Cu_{4.41}Mg_{1.59})Σ₆(Si₄O₁₁)₂(OH)₄. This formula is in fairly good agreement with the empirical ones, considering that the studied crystal fragment was not analysed chemically and the Na content, neglected in the refinement, might be distributed among several of the four *M* sites. The chemically analysed lavinskyite-1*M* fragments contain less Mg (0.36 apfu for Cerch1 and 0.28 apfu for Cerch2) and are somewhat closer to the end-member composition.

The question arises why lavinskyite-1M occurs at the Cerchiara mine and not lavinskyite-2O? The latter appears to be denser, but a complex and delicate interplay between the Li:Cu and Cu:Mg ratios, along with an additional influence of impurity cations such as Na and different conditions of formation (mainly *P*, *T*) may result in a stabilisation of the 1M polytype.

A detailed comparison of the physico-chemical properties of lavinskyite-1M, lavinskyite-2O and plancheite is given in Table 7. The X-ray powder diffraction patterns of both polytypes (Table 6, deposited) are similar, especially in the low-angle region, but distinct differences exist at higher diffraction angles and can be used for identification. We point out that, if the hypothetical $P2_1/c$ MDO equivalent of plancheite (Merlino, 1997) would be found in nature, this would entail a necessary name change to plancheite-1M and plancheite-2O.

Finally, we note that shattuckite $[\text{Cu}_5(\text{SiO}_3)_4(\text{OH})_2]$, Evans & Mrose, 1977; Kawahara, 1976] has a similar sheet-based crystal structure as the two lavinskyite polytypes and plancheite, but its brucite-like $(\text{CuO}_2)_n$ layers have clinopyroxene-type silicate chains joined to them, not amphibole-type chains.

Acknowledgements: The authors thank Fabrizio Castellaro, who found the mineral, for providing samples for study. We also thank Corrado Balestra for some information on the occurrence of the lavinskyite-1M specimens. The article benefited from valuable reviews by two anonymous referees, and editorial assistance by Sergey Krivovichev.

References

- Ashley, P.M. (1986): An unusual manganese silicate occurrence at the Hoskins mine, Grenfell district, New South Wales. *Austr. J. Earth Sci.*, **33**, 443–456.
- Balestra, C. (2005): Norrishite e altre fasi a K-Mn-Si dalla miniera di Cerchiara. *Notiziario di Mineralogia del Ferrania Club*, **19**, 14–16.
- Balestra, C., Kolitsch, U., Blass, G., Callegari, A.M., Boiocchi, M., Armellino, G., Ciriotti, M.E., Ambrino, P., Bracco, R. (2009): Mineralogia ligure 2007–2008: novità caratterizzate dal Servizio UK dell'AMI. *Micro*, **1**, 78–99 (with English abstract).
- Basso, R., Lucchetti, G., Palenzona, A. (1989a): Crystallographic and crystal chemical study on a natural $C2/c$ ordered Na-Mn-clinopyroxene from Val di Vara (northern Apennines, Italy). *N. Jb. Mineral. Mh.*, **1989**, 59–68.
- , —, — (1989b): Orientite and macfallite: new occurrence at the Cerchiara Mine (Eastern Liguria, Italy). *N. Jb. Mineral. Mh.*, **1989**, 455–460.
- Basso, R., Lucchetti, G., Zefiro, L., Palenzona, A. (1993): Mozartite, $\text{CaMn}(\text{OH})\text{SiO}_4$, a new mineral species from the Cerchiara mine, northern Apennines, Italy. *Can. Mineral.*, **31**, 331–336.
- , —, —, — (1997): Caosite, $\text{Ca}(\text{H}_2\text{O})_3(\text{C}_2\text{O}_4)$, a new mineral from the Cerchiara mine, northern Apennines, Italy. *N. Jb. Mineral. Mh.*, **1997**, 84–96.
- , —, —, — (2000): Cerchiaraite, a new natural Ba-Mn-mixed-anion silicate chloride from the Cerchiara mine, northern Apennines, Italy. *N. Jb. Mineral. Mh.*, **2000**, 373–384.
- Basso, R., Cabella, R., Lucchetti, G., Martinelli, A., Palenzona, A. (2005): Vanadiocarpholite, $\text{Mn}^{2+}\text{V}^{3+}\text{Al}(\text{Si}_2\text{O}_6)(\text{OH})_4$, a new mineral from the Molinello mine, northern Apennines, Italy. *Eur. J. Mineral.*, **17**, 501–507.
- Basso, R., Carbone, C., Palenzona, A. (2008): Cassagnaite, a new mineral from the Cassagna mine, northern Apennines, Italy. *Eur. J. Mineral.*, **20**, 95–100.
- Bindi, L., Carbone, C., Cabella, R., Lucchetti, G. (2011): Bassoite, $\text{SrV}_3\text{O}_7 \cdot 4\text{H}_2\text{O}$, a new mineral from Molinello mine, Val Graveglia, eastern Liguria, Italy. *Mineral. Mag.*, **75**, 2677–2686.
- Bindi, L., Carbone, C., Belmonte, D., Cabella, R., Bracco, R. (2013): Weissite from Gambatesa mine, Val Graveglia, Liguria, Italy: occurrence, composition and determination of the crystal structure. *Mineral. Mag.*, **77**, 475–483.
- Cabella, R., Lucchetti, G., Palenzona, A. (1990): Al-rich, Fe-poor manganous sugilite in a pectolite-bearing assemblage from Cerchiara Mine (Northern Apennine, Italy). *N. Jb. Mineral. Mh.*, **1990**, 443–448.
- Cabella, R., Gaggero, L., Lucchetti, G. (1991): Isothermal-isobaric mineral equilibria in braunite-, rhodonite-, johannsenite-, calcite-bearing assemblages from Northern Apennine meta-cherts (Italy). *Lithos*, **27**, 149–154.
- Cabella, R., Lucchetti, G., Palenzona, A., Quartieri, S., Vezzalini, G. (1993): First occurrence of a Ba-dominant brewsterite: structural features. *Eur. J. Mineral.*, **5**, 353–360.
- Cabella, R., Lucchetti, G., Marescotti, P. (1998): Mn-ores from Eastern Ligurian ophiolitic sequences (“Diaspri di Monte Alpe” Formation, Northern Apennines, Italy). *Trends Mineral.*, **2**, 1–17.
- Carbone, C., Basso, R., Cabella, R., Martinelli, A., Grice, J.D., Lucchetti, G. (2013): Mcalpineite from the Gambatesa mine, Italy, and redefinition of the species. *Am. Mineral.*, **98**, 1899–1905.
- Carbone, C., Kolitsch, U., Belmonte, D., Cabella, R., Lucchetti, G., Ciriotti, M.E. (2014): A monoclinic K-Li-Cu-Mg silicate from the Cerchiara mine: a monoclinic dimorph of lavinskyite? 87° Congresso della Società Geologica Italiana & 90° Congresso della Società Italiana di Mineralogia e Petrologia, September 10–12, Milano, Italy. *Rend. Online Soc. Geol. It.*, **31**, Suppl. no. 1, 310.
- Castellaro, F. (2008): 160 volte Cerchiara. *PRIE*, **4**, 114–130.
- Dornberger-Schiff, K. (1964): Grundzüge einer Theorie von OD-Strukturen aus Schichten. *Abhandlungen der Deutschen Akademie der Wissenschaften zu Berlin, Klasse für Chemie, Geologie und Biologie*, **3**, 1–107.
- (1966): Lehrgang über OD-Strukturen. Akademie-Verlag, Berlin.
- Eggleton, R.A. & Ashley, P.M. (1989): Norrishite, a new manganese mica, $\text{K}(\text{Mn}^{3+}_2\text{Li})\text{Si}_4\text{O}_{12}$, from the Hoskins mine, New South Wales, Australia. *Am. Mineral.*, **74**, 1360–1367.
- Evans, H.T., Jr., & Mrose, M.E. (1977): The crystal chemistry of the hydrous copper silicates, shattuckite and plancheite. *Am. Mineral.*, **62**, 491–502.
- Ferraris, G., Makovicky, E., Merlino, S. (2004): Crystallography of molecular materials. Oxford University Press, Oxford, 370 p.
- Fischer, R.X. & Tillmanns, E. (1988): The equivalent isotropic displacement factor. *Acta Crystallogr.*, **C44**, 775–776.
- Gelato, L.M. & Parthé, E. (1987): STRUCTURE TIDY – a computer program to standardize crystal structure data. *J. Appl. Crystallogr.*, **20**, 139–143.
- Gnos, E., Armbruster, T., Villa, I.M. (2003): Norrishite, $\text{K}(\text{Mn}^{3+}_2\text{Li})\text{Si}_4\text{O}_{10}(\text{O})_2$, an oxy mica associated with sugilite from the Wessels Mine, South Africa: crystal chemistry and ^{40}Ar - ^{39}Ar dating. *Am. Mineral.*, **88**, 189–194.

- Guinier, A., Bokij, G.B., Boll-Dornberger, K., Cowley, J.M., Đurovič, S., Jagodzinski, H., Krishna, P., de Wolff, P.M., Zvyagin, B.B., Cox, D.E., Goodman, P., Hahn, T., Kuchitsu, K., Abrahams, S.C. (1984): Nomenclature of polytype structures. Report of the International Union of Crystallography *Ad hoc* Committee on the Nomenclature of Disordered, Modulated and Polytype Structures. *Acta Crystallogr.*, **A40**, 399–404.
- Kampf, A.R., Roberts, A.C., Venance, K.E., Carbone, C., Belmonte, D., Dunning, G.E., Walstrom, R.E. (2013): Cerchiaraita-(Fe) and cerchiaraita-(Al), two new barium cyclosilicate chlorides from Italy and California, USA. *Mineral. Mag.*, **77**, 69–80.
- Kampf, A.R., Carbone, C., Belmonte, D., Nash, B.P., Chiappino, L., Castellaro, F. (2017): Alpeite, $\text{Ca}_4\text{Mn}^{3+}_2\text{Al}_2(\text{Mn}^{3+}\text{Mg})(\text{SiO}_4)_2(\text{Si}_3\text{O}_{10})(\text{V}^{5+}\text{O}_4)(\text{OH})_6$, a new ardennite-group mineral from Italy. *Eur. J. Mineral.*, **29**, 907–914.
- Kawahara, A. (1976): The crystal structure of shattuckite. *Mineral. J.*, **8**, 193–199.
- Kolitsch, U., Carbone, C., Belmonte, D., Cabella, R., Ciriotti, M.E. (2014): Liguriaite, IMA 2014-035. CNMNC Newsletter No. 21, August 2014, p. 803. *Mineral. Mag.*, **78**, 797–804.
- Lacroix, A. (1908): Sur une nouvelle espèce minérale, provenant du Congo français. *Comptes Rendus de l'Académie des Sciences Paris*, **146**, 722–725.
- Lepore, G.O., Bindi, L., Zanetti, A., Ciriotti, M.E., Medenbach, O., Bonazzi, P. (2015): Balestraite, $\text{KLi}_2\text{VSi}_4\text{O}_{10}\text{O}_2$, the first member of the mica group with octahedral V^{5+} . *Am. Mineral.*, **100**, 608–614.
- Lepore, G.O., Bindi, L., Mugnaioli, E., Viti, C., Zanetti, A., Ciriotti, M.E., Bonazzi, P. (2017): A multimethodic approach for the characterization of manganiceladonite, a new member of the celadonite family from Cerchiarra mine, Eastern Liguria, Italy. *Mineral. Mag.*, **81**, 167–173.
- Lucchetti, G., Penco, A.M., Rinaldi, R. (1981): Saneroite, a new natural hydrated Mn-silicate. *N. Jb. Mineral. Mh.*, **1981**, 161–168.
- Lucchetti, G., Cortesogno, L., Palenzona, A. (1988): Low-temperature metamorphic mineral assemblages in Mn-Fe ores from Cerchiarra mine (northern Apennine, Italy). *N. Jb. Mineral. Mh.*, **1988**, 367–383.
- Ma, C., Carbone, C., Belmonte, D. (2014): Cortesognoite, IMA2014-029. CNMNC Newsletter No. 21, August 2014, page 801. *Mineral. Mag.*, **78**, 797–804.
- Mandarino, J.A. (1981): The Gladstone-Dale relationship: Part IV. The compatibility concept and its application. *Can. Mineral.*, **19**, 441–450.
- Merlino, S. (Ed.) (1997): Modular aspects of minerals. “EMU notes in Mineralogy 1”. Eötvös University Press, Budapest, 448 p.
- Moore, J.M., Kuhn, B.K., Mark, D.F., Tsikos, H. (2011): A sugilite-bearing assemblage from the Wolhaarkop breccia, Bruce iron-ore mine, South Africa: evidence for alkali metasomatism and ^{40}Ar - ^{39}Ar dating. *Eur. J. Mineral.*, **23**, 661–673.
- Otwinowski, Z., Borek, D., Majewski, W., Minor, W. (2003): Multiparametric scaling of diffraction intensities. *Acta Crystallogr.*, **A59**, 228–234.
- Palenzona, A. & Selmi, P. (1990): La sugilite di Cerchiarra (SP). *Rivista Mineral. Ital.*, **3**, 153–154.
- Palenzona, A., Di Giovanni, F., Borgo, E. (1988): La miniera di Manganese di Cerchiarra (SP). *Rivista Mineral. It.*, **4**, 209–218.
- Shape Software (2006) ATOMS for Windows and Macintosh V6.3. Kingsport, TN 37663, USA.
- Sheldrick, G.M. (2008): A short history of *SHELX*. *Acta Crystallogr.*, **A64**, 112–122.
- Spek, A.L. (2003): Single-crystal structure validation with the program *PLATON*. *J. Appl. Crystallogr.*, **36**, 7–13.
- Spek, A.L. (2009): Structure validation in chemical crystallography. *Acta Crystallogr.*, **D65**, 148–155.
- Tsikos, H. & Moore, J.M. (2005a): Structure validation in chemical crystallography. *Acta Crystallogr.*, **D65**, 148–155.
- , — (2005b): Sodic metasomatism in the Paleoproterozoic Hotazel iron-formation, Transvaal Supergroup, South Africa: implications for fluid-rock interaction in the Kalahari manganese field. *Geofluids*, **5**, 264–271.
- Wenger, M. & Armbruster, T. (1991): Crystal chemistry of lithium: Oxygen coordination and bonding. *Eur. J. Mineral.*, **3**, 387–399.
- Yang, H., Downs, R.T., Evans, S.H., Pinch, W.W. (2014): Lavinskyite, $\text{K}(\text{LiCu})\text{Cu}_6(\text{Si}_4\text{O}_{11})_2(\text{OH})_4$, isotypic with plancheite, a new mineral from the Wessels mine, Kalahari Manganese Fields, South Africa. *Am. Mineral.*, **99**, 525–530.

Received 3 May 2017

Modified version received 18 June 2017

Accepted 20 June 2017